Indian J.Sci.Res. 17 (1): 245-249, 2017 ISSN: 0976-2876 (Print)
ISSN: 2250-0138 (Online)

ENHANCING MECHANICAL RESPONSE OF MAGNESIUM USING YTTRIUM AND YTTRIUM OXIDE

AYUSH RAI[a1], SRAVYA TEKUMALLA[b], GURURAJ PARANDE[c], VYASARAJ MANAKARI[d], MILLI SUCHITA KUJUR[e], KHIN SANDAR TUN[f] AND MANOJ GUPTA[g]

[a]Department of Mechanical Engineering, Indian Institute of Technology Delhi, New Delhi, India
[bcdfg]Department of Mechanical Engineering, National University of Singapore, 9 Engineering Drive 1, Singapore
[e]Department of Mechanical Engineering, Indian School of Mines, Dhanbad, Jharkhand, India

ABSTRACT

Strong and lightweight materials are the need of the hour for the weight critical industries such as aerospace and the automotive sectors. Magnesium with high specific strength is the lightest structural metal available on earth. However, its industrial application is restricted because of its limited ductility under tensile loads, poor elastic modulus, and low creep resistance at higher temperatures. This study aims to investigate the effect of yttrium and yttrium oxide nanoparticles on the mechanical response of pure magnesium. Magnesium-yttrium binary alloy and its nanocomposite with yttrium oxide as reinforcement were casted using disintegrated melt deposition technique at 750^{o}C followed by hot extrusion. The binary alloy and nanocomposite were subsequently characterized for their microstructural and mechanical properties and were compared with pure magnesium. The mechanical behavior tested in compression demonstrated progressive increase in strength after addition of yttrium and yttrium oxide. On contemplation, relationship between microstructure of the engineered composite and mechanical properties was established.

KEYWORDS: Magnesium-Yttrium Alloy, Yttrium Oxide, Nanoreinforcement, Disintegrated Melt Deposition, Mechanical Properties.

Magnesium (Mg), being one of the lightest engineering and structural metals available on the earth shows excellent damping capacity and high specific mechanical strength [1]. Magnesium has a density of 1.74 g/cm^3, which is 35% lighter than aluminium (2.7 g/cm^3) and over four times lighter than steel (7.86 g/cm^3) [2]. Besides low density, ease of fabrication and it's capability to withstand elevated temperatures had made Mg an attractive choice for aerospace industry [3]. However, despite these advantages, it's application remains limited because of its low ductility, poor elastic modulus, and low corrosion and creep resistance [4].

Effect of yttrium and yttrium oxide (Y_2O_3) on magnesium has been extensively studied, individually and it has shown promising increase in strength and ductility [5], [6]. Goh et al. reported improvement in physical and tensile properties for as-extruded Mg-Y_2O_3 nanocomposites [6]. No research has been done yet to study the effect of reinforcement (Y_2O_3) on Mg-Y alloys.

In the present study, monolithic Mg, a binary alloy (Mg+1.8Y) and binary alloy with nanoreinforcement (Mg+1.8Y+1.5Y_2O_3) were synthesized through disintegrated melt deposition technique followed by hot extrusion. The alloys were characterized in terms of their microstructural, physical and mechanical properties. Structure-property relation has been studied, analyzed and established. The developed materials are aimed to suit the applications in aerospace industry, specifically for interiors of combat aircrafts.

MATERIALS AND EXPERIMENTAL PROCEDURE

Materials

For the study, Mg turnings of 99.9% purity were supplied by ACROS Organics, USA. Mg-30Y master alloy was used instead of pure Yttrium. Mg-30Y master alloy with 99% purity and Yttrium Oxide (Y_2O_3) of 29nm size with 99.9% purity were sourced from Sunrelier Metal Co. Limited, China.

Synthesis of Mg-Y-Y_20_3 alloys

Monolithic Mg, Mg+1.8Y and Mg+1.8Y+1.5Y_2O_3 (wt. %) were casted using disintegrated melt deposition (DMD) technique. In a graphite crucible, Mg turnings along with Mg-30Y master alloy and Y_2O_3 powder were heated up to 750^{0}C in an electrical resistance furnace under inert argon gas protective atmosphere. Once superheated, the molten slurry was stirred at 465 rpm for 5 min. using a twin blade (pitch 450) mild steel impeller to facilitate the uniform distribution of heat. The melt was then released through an orifice at the bottom of the crucible and was disintegrated using two jets of argon gas oriented normal to the melt stream. An ingot of 40 mm diameter was obtained after deposition. The obtained ingot was then machined to billets of diameter 35 mm followed by hot

[1]Corresponding author

extrusion at 350^0C with extrusion ratio 20.25:1. Rods of 8 mm diameter were obtained which were used for characterization and analysis.

Characterization of Mg-Y- Y_2O_3 alloys

Microstructural Characterization

Grain Morphology

The grain size and morphology of monolithic Mg and its composite were studied using their optical micrographs captured by LEICA -DM 2500M Metallographic Optical Microscope. The longitudinally cut samples were polished and etched to reveal grain boundaries. The grain size measurement was accomplished with the help of Scion image analysis software.

Secondary Phase Analysis

The distribution of secondary phases was analyzed using scanning electron microscope (JEOL JSM-6010) along with energy dispersive spectrometric analysis (EDS) on mirror polished samples of composites. Images were captured at an accelerating voltage of 15 kV, working distance of approximately 16 mm and emission current of 41 μA.

Physical Characterization

Density and Porosity

Archimedes' principle was used for density measurement. The samples were weighed in air and then in distilled water using an A&D GR-200 electronic balance with an accuracy of ±0.0001g. The results were confirmed using pycnometer. Rule of mixtures was used to calculate theoretical densities of the alloys and the difference between the theoretical and experimental densities were quantified with porosity values.

Coefficient of Thermal Expansion

Coefficient of Thermal Expansion (CTE) values were measured using thermomechanical analyzer (INSEIS TMA PT 1000LT). Alumina probe measured the displacement of the samples as a function of temperature with heating rate of 50C/min and argon flow rate of 0.1 lpm.

Damping

Damping capacity was tested using resonant frequency and damping analyzer (RFDA) from IMCE. Test was conducted in accordance with ASTM standard E1876-09.

Mechanical Characterization

Micro-Hardness

Micro-Hardness values were measured using Shimadzu HMV automatic digital microhardness tester with a Vickers indenter (square-based pyramidal-shaped diamond indenter with a face angle of 136^0). Indent was made with a load of 25gf for dwell time of 15s. Test was performed on mirror polished samples in accordance with ASTM standard E384-11e1.

Compression

Measurements of compressive strength were done using a fully automated servo-hydraulic mechanical testing machine, Model-MTS810 in accordance with ASTM standard E9-09. With cross head speed 0.04 mm/min and strain rate of 8.334×10^{-5} s^{-1}, specimens with length to diameter ratio around 1 were tested. Fractography studies were made on fractured samples using JEOL JSM-5600LV Scanning Electron Microscope.

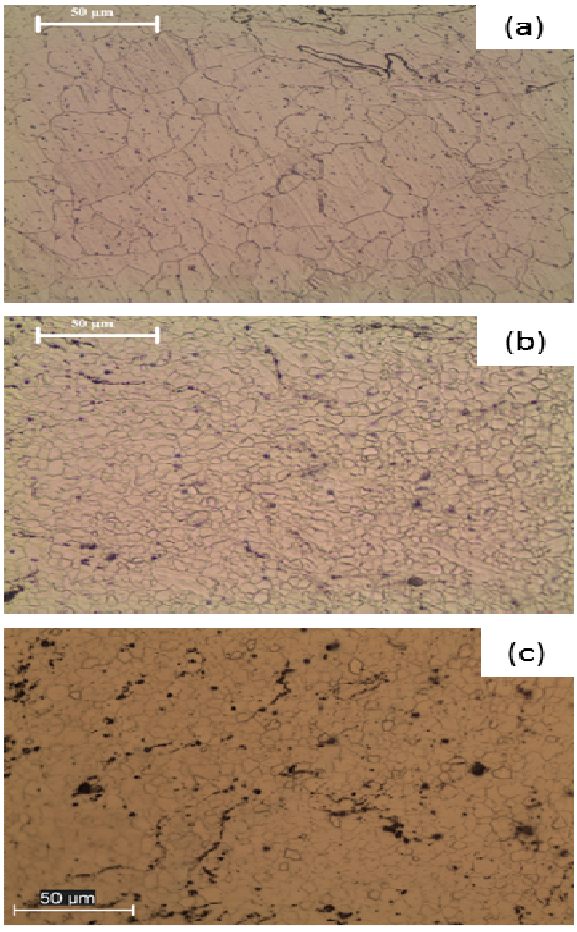

Figure 1: Grain size measurement under optical microscope for (a) Pure Mg (b) Mg+1.8Y (c) Mg+1.8Y+1.5Y_2O_3

RESULTS AND DISCUSSION

Microstructural Characterization

Grain Morphology

Figure 1 shows the optical micrographs of the compositions. Equiaxed grains indicate a complete recrystallization that has taken place during the extrusion [7]. The grain size values are tabulated in Table 1. Reduction in grain diameter was observed after addition of Y and Y_2O_3 by 79.62% and 70.61%.

Secondary Phase Analysis

SEM micrographs, shown in Figure 2, indicate the presence of secondary phases Mg_2Y and $Mg_{24}Y_5$ in Mg+1.8Y. In Mg+1.8Y+1.5Y_2O_3, Mg_2Y as second phase and Y_2O_3 as reinforcement were encountered. $Mg_{24}Y_5$ phase observed along the grain boundary in Mg+1.8Y that led to grain refinement through grain boundary pinning effects was not seen in the current magnifications in Mg+1.8Y+1.5Y_2O_3 [8]. Further, extensive study must be done for the conclusive findings of the secondary phase in the nanocomposite.

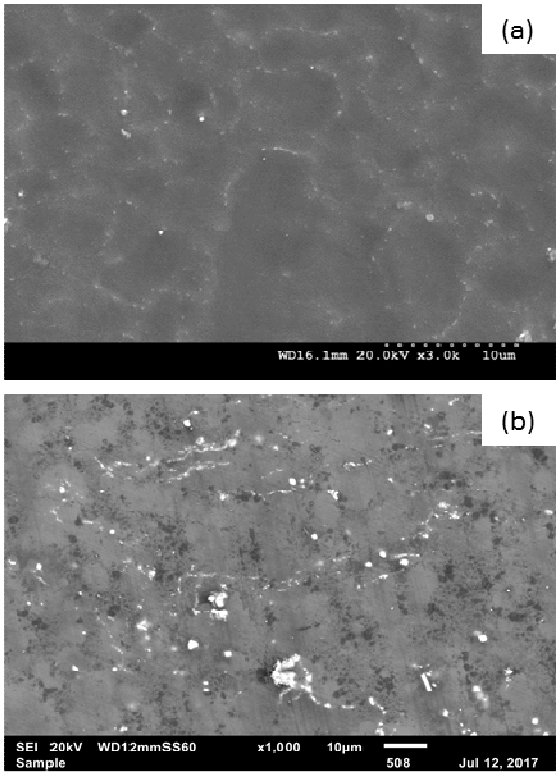

Figure 2: Secondary phase studies using SEM of (a) Mg + 1.8Y (b) Mg + 1.8Y + 1.5Y_2O_3

Physical Characterization

Density and Porosity

Measurements indicated in Table 1 show that both theoretical and experimental densities increase with subsequent addition of Y and Y_2O_3. Porosity values do not follow any general trend. High porosity of Mg+1.8Y+1.5Y_2O_3 when compared to Mg+1.8Y is possibly attributed to clustering effect because of addition of nanoreinforcement.

Coefficient of Thermal Expansion

The CTE values measured over the temperature range of 100 to 400°C are provided in Table 2. The lower the value of CTE, the lesser is the tendency for the material to change shape with change in temperature. The binary alloy showed a slight increase in CTE value but a decrement of 20.47% is observed with the addition Y_2O_3 as nanoreinforcement. Hence Mg+1.8Y+1.5 Y_2O_3 turns out to be most thermally stable material.

Table 1: Results of grain size diameter, experimental and theoretical density and porosity.

Material (wt. %)	Grain size (µm)	Theoretical Density (g/cc)	Experimental Density (g/cc)	Porosity (%)
Pure Mg	21.1 ± 1.9	1.738	1.712 ± 0.017	1.46
Mg + 1.8 Y	4.3 ± 0.2	1.757	1.739 ± 0.026	1.04
Mg + 1.8 Y + 1.5 Y_2O_3	6.2 ± 1.9	1.774	1.749 ± 0.004	1.38

Table 2: Coefficient of thermal Expansion (CTE) and microhardness values.

Material (wt. %)	Coefficient of Thermal Expansion (K^{-1})	Micro-Hardness (Hv)
Mg	25.55×10^{-6}	66 ± 3
Mg + 1.8 Y	26.33×10^{-6}	85 ± 4 (↑ 28.8%)
Mg + 1.8 Y + 1.5 Y_2O_3	20.32×10^{-6}	74 ± 5 (↑ 12.1%)

Damping

The amplitude versus time curves obtained from damping test is presented in Figure 3. Improved damping capacity was observed with time required to stop the vibration decreasing subsequently for Mg+1.8Y and Mg+1.8Y+1.5Y_2O_3 from 0.8s to 0.27s and 0.2s respectively.

Mechanical Characterization

Micro-Hardness

The average values of various measurements made for microhardness are given in table 2. Table 2 highlights the increment in microhardness for Mg+1.8Y and Mg+1.8Y+1.5Y_2O_3 by 28.8% and 12.1% respectively. Large increment in case of Mg+1.8Y can be attributed to grain refinement and formation of secondary phase $Mg_{24}Y_5$.

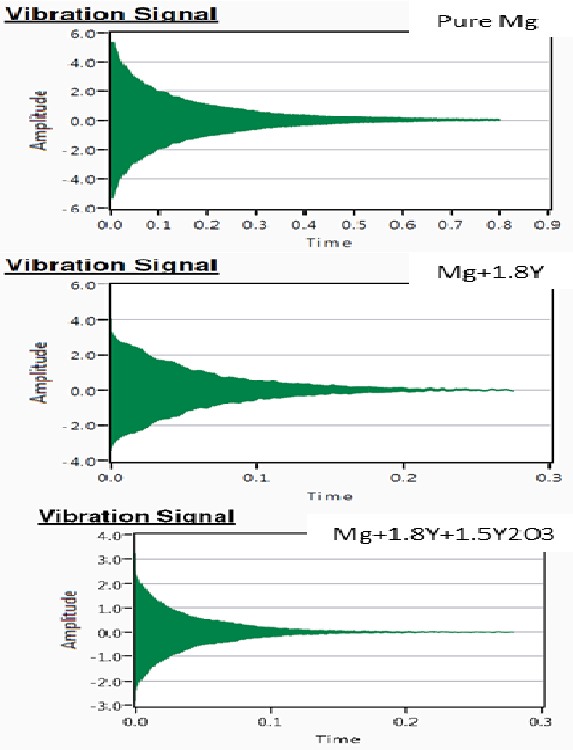

Figure 3: Damping characteristics of the materials.

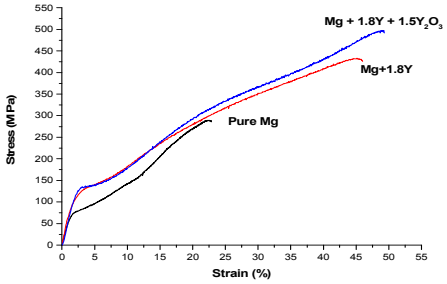

Figure 4: Engineering compressive stress-strain curves.

Compressive Response

The compressive behavior of the materials is given in Table 3. Addition of Y and Y_2O_3 has progressively increased the value of 0.2% yield strength, ultimate compressive strength, ductility and energy absorbed. The binary alloy in comparison with monolithic Mg marked an increment of 56% and 46% for 0.2% and ultimate compressive strength, respectively. These values for the nanocomposite (Y_2O_3) increased to 98.5% and 61.5% respectively indicating Mg+1.8Y+1.5Y_2O_3 to be more ductile with higher strength. It is interesting to note that ultimate compressive strength of Mg+1.8Y+1.5Y_2O_3 was as high as 499MPa.

Table 3: Results of compressive tests.

Material (wt. %)	0.2% yield strength (MPa)	Ultimate tensile strength (MPa)	Fracture Strain (%)	Energy absorbed (MJ/m3)
Mg	66 ± 4	309 ± 14	23 ± 2.5	41 ± 3.9
Mg + 1.8 Y	103 ± 4	449 ± 22	48 ± 2.5	143 ± 9.6
Mg + 1.8 Y + 1.5 Y_2O_3	131 ± 2	499 ± 14	48 ± 1.5	149.7 ± 5.8

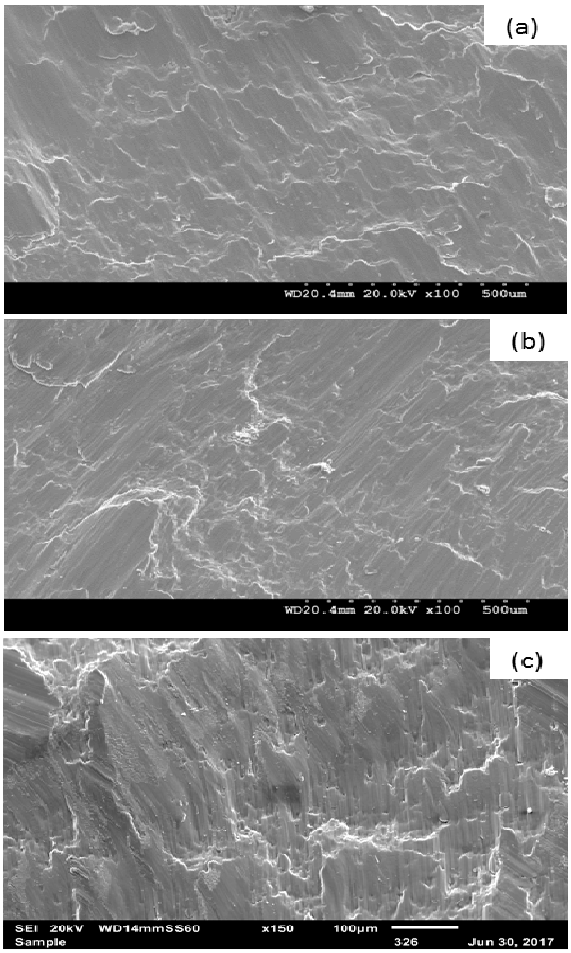

Figure 5: Fractography results for (a) Pure Mg (b) Mg + 1.8Y (c) Mg + 1.8Y + 1.5Y_2O_3.

Enhancement in mechanical properties (Fig. 4) can be attributed to the microstructural features. In both the alloy and nanocomposite, strengthening due to grain size reduction and formation of equiaxed grain along with secondary phases has taken place. Mg+1.8Y+1.5Y_2O_3 shows more improvement due to presence of Y_2O_3 as nanoreinforcement.

Figure 5 shows the SEM images of compressive fractures. Shear bands were formed at angle of 45^0 indicating that failure in composites were driven by matrix material.

CONCLUSION

With an aim to understand and compare the effect of alloying and adding nanoreinforcement with rare earth metal, monolithic Mg, Mg+1.8Y and Mg+1.8Y+1.5Y_2O_3 were synthesized through disintegrated melt deposition technique followed by hot extrusion. From the characterization and analysis of the compositions following conclusions can be drawn-

1. Addition of Y and Y_2O_3 led to development of refined microstructure with equiaxed grains.
2. Addition of Y_2O_3 reduced the CTE value up to 20.32 μK^{-1}, resulting in more dimensionally stable nanocomposites.
3. Mg+1.8Y in comparison to Mg+1.8Y+1.5Y_2O_3 showed higher resistance to microhardness indenter. This is due to formation of secondary phases.
4. Alloying and addition of reinforcement result in gradual enhancement in damping capacity.
5. Remarkable increase of 98.5% for 0.2% yield strength is achieved for Mg+1.8Y+1.5Y_2O_3 relative to monolithic Mg. This rise can be attributed due to presence of secondary phases and Y_2O_3 nanoreinforcement.

REFERENCES

M. E. Alam, S. Han, Q. B. Nguyen, A. M. Salem Hamouda, and M. Gupta, "Development of new magnesium based alloys and their nanocomposites," J. Alloys Compd., vol. 509, no. 34, pp. 8522–8529, 2011.

M. K. Kulekci, "Magnesium and its alloys applications in automotive industry," Int. J. Adv. Manuf. Technol., vol. 39, no. 9–10, pp. 851–865, 2008.

M. (Manoj) Gupta and M. L. S. Nai, Magnesium, magnesium alloys, and magnesium composites : a guide. Wiley, pp. 7-8, 2011.

M. M. Avedesian, H. Baker, and ASM International. Handbook Committee., Magnesium and magnesium alloys. ASM International, pp. 7-11, 1999.

S. Tekumalla et al., "Enhancing overall static/dynamic/damping/ignition response of magnesium through the addition of lower amounts (<2%) of yttrium," J. Alloys Compd., vol. 689, no. October, pp. 350–358, 2016.

C. S. Goh, J. Wei, L. C. Lee, and M. Gupta, "Properties and deformation behaviour of Mg-Y2O3 nanocomposites," Acta Mater., vol. 55, no. 15, pp. 5115–5121, 2007.

R. . Davies, V. Randle, and G. . Marshall, "Continuous recrystallization—related phenomena in a commercial Al–Fe–Si alloy," Acta Mater., vol. 46, no. 17, pp. 6021–6032, 1998.

J. D. Robson, D. T. Henry, and B. Davis, "Particle effects on recrystallization in magnesium-manganese alloys: Particle pinning," Mater. Sci. Eng. A, vol. 528, no. 12, pp. 4239–4247, 2011.